

# 1 **Metabolic complementarity between a brown alga and associated** 2 **cultivable bacteria provide indications of beneficial interactions.**

3 **Bertille Burgunter-Delamare<sup>1†</sup>, Hetty KleinJan<sup>1‡</sup>, Clémence Frioux<sup>2</sup>, Enora Fremy<sup>2</sup>, Margot**  
4 **Wagner<sup>2</sup>, Erwan Corre<sup>3</sup>, Alicia Le Salver<sup>3</sup>, Cédric Leroux<sup>3</sup>, Catherine Leblanc<sup>1</sup>, Catherine**  
5 **Boyen<sup>1</sup>, Anne Siegel<sup>2</sup>, Simon M. Dittami<sup>1\*</sup>**

6 <sup>1</sup> Sorbonne Université, CNRS, Integrative Biology of Marine Models (LBI2M), Station Biologique  
7 de Roscoff, 29680 Roscoff, France

8 <sup>2</sup> Univ Rennes, Inria, CNRS, IRISA, Rennes F-35000, France

9 <sup>3</sup> Sorbonne Université, CNRS, FR2424, Station Biologique de Roscoff, 29680, Roscoff, France

10 ‡ present address: CEBEDEAU, Research and Expertise Center for Water, Allée de la découverte, 11  
11 (B53), Quartier Polytech 1, B-4000, Liège, Belgium.

12 † These authors contributed equally to this study.

## 13 **\* Correspondence:**

14 Corresponding Author

15 [simon.dittami@sb-roscoff.fr](mailto:simon.dittami@sb-roscoff.fr)

16 **Keywords: *Ectocarpus siliculosus*, symbiotic/mutualistic bacteria, genome-scale metabolic**  
17 **networks, metabolic complementarity, holobiont**

## 18 **Abstract:**

19 Brown algae are key components of marine ecosystems and live in association with bacteria that are  
20 essential for their growth and development. *Ectocarpus siliculosus* is a genetic and genomic model  
21 for brown algae. Here we use this model to start disentangling the complex interactions that may  
22 occur between the algal host and its associated bacteria. We report the genome-sequencing of 10  
23 alga-associated bacteria and the genome-based reconstruction of their metabolic networks. The  
24 predicted metabolic capacities were then used to identify metabolic complementarities between the  
25 algal host and the bacteria, highlighting a range of potentially beneficial metabolite exchanges  
26 between them. These putative exchanges allowed us to predict consortia consisting of a subset of  
27 these ten bacteria that would best complement the algal metabolism. Finally, co-culture experiments  
28 were set up with a subset of these consortia to monitor algal growth as well as the presence of key  
29 algal metabolites. Although we did not fully control but only modify bacterial communities in our  
30 experiments, our data demonstrated a significant increase in algal growth in cultures inoculated with  
31 the selected consortia. In several cases, we also detected, in algal extracts, the presence of key  
32 metabolites predicted to become producible via an exchange of metabolites between the alga and the  
33 microbiome. Thus, although further methodological developments will be necessary to better control  
34 and understand microbial interactions in *Ectocarpus*, our data suggest that metabolic  
35 complementarity is a good indicator of beneficial metabolite exchanges in holobiont.

## 36 **1 Introduction**

37 Microbial symbionts are omnipresent and important for the development and functioning of  
38 multicellular eukaryotes. Together the eukaryote hosts and their microbiota form meta-organisms  
39 also called holobionts. Elucidating the interactions within microbial communities and how they affect  
40 host physiology is a complex task and requires an understanding of the dynamics within the  
41 microbiome and the host, as well as of possible inter-species interactions and/or metabolic exchanges  
42 that could occur between the partners. One way to dissect those interactions is via targeted co-culture  
43 experiments using culturable bacteria. This approach works particularly well for 1:1 or 1:2  
44 interactions, but as the number of potentially interacting organisms increases, selecting the “right”  
45 bacterial consortia becomes a major bottleneck (Lindemann *et al.* 2016).

46 Metabolic complementarity has previously been proposed as an indicator for potentially beneficial  
47 host-symbiont interactions and can be assessed *in silico* using the metabolic networks of the host and  
48 the microbiota (Dittami, Eveillard, *et al.* 2014; Levy *et al.* 2015). Common examples of metabolic  
49 complementarity are associations of autotrophic and heterotrophic organisms such as corals and their  
50 photosynthetic symbionts (Rohwer *et al.* 2002), or algae, and their heterotrophic bacterial biofilm  
51 (Wahl *et al.* 2012). In this case, the autotrophic partner has a metabolic capacity (photosynthesis) that  
52 allows for the production of metabolic intermediates (organic carbon), which can be further  
53 metabolized by the heterotrophic partners. However, especially in systems with long-lasting  
54 interactions more complex metabolic interdependencies are likely to evolve (*e.g.* Amin *et al.* 2015).

55 As a tool to further explore such interactions, Frioux *et al.* (Frioux *et al.* 2018) have proposed the  
56 pipeline MiSCoTo. Given the metabolic networks of a host and several symbionts, this tool predicts  
57 potential metabolic capacities of one partner that could be unlocked by a contribution of a metabolite  
58 from another (*e.g.* the provision of carbohydrates by a photosynthetic organism unlocking the  
59 biochemical processes related to primary metabolism in heterotrophs). Furthermore, this  
60 computational approach uses these complementarities to define minimal consortia (*i.e.* with the  
61 lowest possible number of exchanges/contributors) allowing the host to reach its maximum metabolic  
62 potential. However, the actual predictive value of these models, both in terms of the effect on host  
63 growth and fitness, and in terms of the metabolic scope (*i.e.* the metabolites producible by the  
64 holobiont system), remains to be assessed.

65 Here we have applied the MiSCoTo tool to the filamentous brown alga *Ectocarpus siliculosus*, a  
66 model filamentous brown alga with an available metabolic network (Prigent *et al.* 2014), as well as a  
67 selection of 10 *Ectocarpus*-derived bacteria (KleinJan *et al.* 2017). We then selected specific minimal  
68 microbial consortia for *in vivo* testing of the proposed hypotheses (growth rate, production of specific  
69 metabolites). Our results demonstrate a clear positive effect of inoculation with the predicted  
70 bacterial consortia on algal growth as well as an effect on the production of algal metabolites  
71 predicted to depend on bacterial contributions. *In vivo* observations largely corresponded to *in silico*  
72 predictions despite the incomplete input data (with models limited to annotated pathways) and the  
73 fact that we had only limited control of the microbiome. The present work thus generates numerous  
74 testable hypotheses on specific beneficial interactions between *Ectocarpus* and its microbiome, but  
75 also provides a proof of concept for the overall predictive power of network-based metabolic  
76 complementarity for beneficial host-microbe interactions.

## 77 **2 Methods**

### 78 **2.1 Bacterial cultures and genome sequencing**

79 Ten bacterial strains were selected from the 46 isolated by KleinJan et al. from *Ectocarpus subulatus*  
80 (KleinJan et al. 2017). They were grown in liquid Zobell and/or diluted R2A until bacterial growth  
81 was visible with the naked eye (~3 days at room temperature), and their identity was confirmed by  
82 sequencing of the 16S rRNA gene with the primers 8F and 1492R (KleinJan et al. 2017). Bacterial  
83 DNA was extracted using the UltraClean® Microbial DNA isolation kit (MoBio, Qiagen, Hilden,  
84 Germany) and used for standard pair-end sequencing at the GENOMER platform (FR2424, Station  
85 Biologique de Roscoff), using Illumina Miseq technology (V3 chemistry, 2x300bp). After cleaning  
86 with Trimmomatic v0.38, default parameters (Bolger et al. 2014), the paired-end reads were  
87 assembled using SPADes v3.7.0 (Bankevich et al. 2012; default parameters for long reads). The  
88 RAST/SEED server (Aziz et al. 2008) was used for gene annotation, and sequences were later also  
89 incorporated into the MAGE platform (Vallenet et al. 2006).

## 90 **2.2 In silico predictions of metabolic interactions and selection of consortia**

91 Bacterial metabolic networks were constructed using Pathway Tools version 20.5 (Karp et al. 2016)  
92 and version 2 of the *Ectocarpus siliculosus* EC32 metabolic network for the host, prior to any gap-  
93 filling step, in order to prevent the presence of possibly false positive reactions in the model.  
94 (because these false positive reactions could hide algal bacterial interactions). This network  
95 comprised a total of 2,118 metabolites, 1,887 metabolic reactions, and was able to produce five of the  
96 50 metabolites known to be a part of the *Ectocarpus* biomass (Aite et al. 2018) with only the culture  
97 medium as input. For the remaining 45 compounds the lack of producibility can be explained by the  
98 presence of metabolic gaps – either because a reaction was missed during the reconstruction of the  
99 network (missing annotation etc.), or because the corresponding pathways require metabolite  
100 exchanges with other partners in the environment, e.g. bacteria. The more such gaps can be filled by  
101 exchanging compounds between two metabolic networks, the higher we consider the degree of  
102 metabolic complementarity between the corresponding organisms.

103 Here we used the MiSCoTo tool (Frioux et al. 2018) to compute such potential metabolic exchanges  
104 between *Ectocarpus* and any of the ten targeted bacteria. The underlying model of MiSCoTo  
105 assumes that a compound is producible by a host-symbiont community if there is a chain of  
106 metabolic reactions which transforms the culture medium into the expected compound without taking  
107 into consideration flux accumulations or competition for resources, and allowing for the exchange of  
108 compounds across cell boundaries. These simplifications imply that compounds predicted to be  
109 producible *in silico* may, in some cases, remain unproducible *in vivo*, although the consortium has all  
110 the genes to activate the pathways.

111 In this study MiSCoTo was run twice, first to determine the scope of all algal compounds that  
112 become producible via exchanges with all 10 bacterial genomes together, and as second time to select  
113 minimal bacterial consortia for the production of these compounds. In both cases the Provasoli  
114 culture medium was used as a source as defined previously (Prigent et al. 2014).

## 115 **2.3 Algal cultures**

116 Two of the six predicted bacterial consortia were tested experimentally via algal-bacterial co-culture  
117 experiments. Additionally, each member of the two consortia was tested individually, as well one  
118 other sequenced strain that was not part of any of the predicted minimal consortia, i.e. *Sphingomonas*  
119 sp. 391. *Ectocarpus siliculosus* (strain 32; accession CCAP 1310/4, origin San Juan de Marcona,  
120 Peru) was cultured under standard conditions (13 °C; 12h light regime) in Provasoli-enriched natural  
121 seawater until the start of antibiotic treatment. Prior to co-culture experiments, algal filaments were  
122 treated with a mixture of the following liquid antibiotics: 45 µg/ml Penicillin G, 22.5 µg/ml

123 streptomycin, and 4.5 µg/ml chloramphenicol dissolved in Provasoli-enriched artificial seawater 450  
124 mM Na<sup>+</sup>, 532 mM Cl<sup>-</sup>, 10 mM K<sup>+</sup>, 6 mM Ca<sup>2+</sup>, 46 mM Mg<sup>2+</sup>, 16 mM SO<sub>4</sub><sup>2-</sup>. Filaments were exposed  
125 to 25 ml of this solution for 3 days and then placed in Provasoli-enriched artificial seawater for 3  
126 days to recover. The absence of bacteria on the algal surface was verified by microscopy using phase-  
127 contrast (Olympus BX60, 1.3- PH3 immersion objective, 800x magnification) and by plating of algal  
128 filaments on Petri dishes with Zobell medium followed by three weeks of incubation at room  
129 temperature.

## 130 **2.4 Co-culture experiments**

131 For co-culture experiments, cell densities of bacterial cultures were determined using a BD FACS  
132 Canto<sup>TM</sup> II flow cytometer (BD Bioscience, San Jose, CA) using samples fixed in Tris-EDTA.  
133 Before the start of the experiment, antibiotic-treated algae (three replicate cultures per condition)  
134 were inoculated with 2.3\*10<sup>5</sup> bacterial cells per strain and ml medium. Each co-culture was then  
135 incubated for 4 weeks under standard algal growth conditions (see above). During this time, algal  
136 growth was quantified by measuring the filament length of the algae each week using the binocular  
137 microscope (3 measurements per replicate). Furthermore, bacterial abundance in the algal growth  
138 medium was estimated using flow cytometry (described above) and bacteria attached to algal cell  
139 walls were counted by microscopy (5x 10 µm long filaments observed per biological replicate, 800x  
140 magnification in phase contrast). At the end of the experiment, general algal morphology was  
141 observed using a LEICA DMI8 microscope and in parallel, remaining algal tissues were frozen in  
142 liquid nitrogen and freeze-dried for downstream analyses. Two controls (three replicates each) were  
143 run in parallel: a non-antibiotic treated positive control (CTRL w/o. ATB), and an antibiotic-treated  
144 non-inoculated alga as a negative control (CTRL w. ATB).

## 145 **2.5 Bacterial community composition after co-culture experiments**

146 A metabarcoding approach was implemented to investigate the composition of the bacterial  
147 community after the co-culture experiments. For each culture, 20 mg ground freeze-dried tissue  
148 (TissueLyserII Qiagen, Hilden, Germany; 2x45sec, 30 Hz) was used for DNA extraction (DNeasy  
149 Plant Mini Kit, Qiagen; standard protocol). Nucleotide concentrations were verified with  
150 NanodropONE (ThermoFisher Scientific). A mock community comprised of DNA from 32 bacterial  
151 strains (covering a variety of taxa) as well as a negative control were included in addition to the  
152 samples (see Thomas *et al.* in prep. for details). Libraries were prepared according to the standard  
153 Illumina protocol for metabarcoding MiSeq technology targeting the V3–V4 region (Illumina 2017)  
154 and sequenced using Illumina MiSeq Technology (2x300 bp, pair-end reads; MiSeq Reagent v3 kit;  
155 Platform de Séquencage-Génotypage GENOMER, FR2424, Roscoff).

156 Resulting raw sequences (7,354,164 read pairs) were trimmed using fastq\_quality\_trimmer from the  
157 FASTX Toolkit (quality threshold 30; minimum read length 200) and assembled into 6,804,772  
158 contigs using PandaSeq v2.11 (Masella *et al.* 2012). Data were analyzed with Mothur (V.1.40.3)  
159 according to the MiSeq Standard Operating Procedures (Kozich *et al.* 2013). Contigs were pre-  
160 clustered (allowing for four mismatches), and aligned to the Silva\_SEED 132b database for sequence  
161 classification. Chimeric sequences were removed (Vsearch) and the remaining sequences classified  
162 taxonomically (Wang *et al.* 2007). Non-bacterial sequences were removed and the remaining  
163 sequences were then clustered into operational taxonomic units (OTUs) at a 97% identity level and  
164 each OTU was classified to the genus level where possible (Wang *et al.* 2007). All OTUs with n ≤ 10  
165 sequences were removed resulting in a final data matrix with 1,834,992 sequences. The OTU matrix  
166 was subsampled to have the same number of sequences per sample for downstream analyses.

## 167 **2.6 Targeted metabolomics**

168 Seven metabolites predicted to be producible by the algae only in presence of metabolic exchanges  
169 with specific bacteria were selected for targeted metabolite profiling after manual verification of  
170 automatic predictions of corresponding pathways in the algal and bacterial networks and based on  
171 their biological importance for the alga: L-histidine, putrescine, beta-alanine, nicotinic acid, folic  
172 acid, auxin, and spermidine. Metabolites were extracted from 10 mg of ground, freeze-dried tissue  
173 using a triple extraction protocol based on the method of Bligh and Dyer (1959): two ml of  
174 methanol:chloroform:water (6:4:1) were used as first extraction solvent, then the remaining pellet  
175 was extracted with 1 ml of chloroform:methanol (1:1), and finally, a 3rd extraction was performed  
176 using 1ml of H<sub>2</sub>O. The supernatants of each extraction were pooled and evaporated under a stream of  
177 nitrogen. The residue was then resuspended in 100 µl methanol:water (1:1) and analyzed on an  
178 ACQUITY Ultra-performance convergence chromatography (UPC<sup>2</sup>) system (Waters®, Milford,  
179 USA) equipped with a Viridis BEH column (3x100 mm, 1.7 µm). A linear gradient of two solvents  
180 was used to separate peaks: supercritical carbon dioxide (Solvent A), and methanol spiked with 0.1%  
181 formic acid (Solvent B). The gradient ran from 5% to 25% of solvent B (35% for spermidine and  
182 nicotinic acid) during 2 minutes, was kept at this level for another 2 minutes and then gradually  
183 reduced back to 5% during 3 minutes. The UPC<sup>2</sup> system was coupled to a Xevo G2 Q-Tof mass  
184 spectrometer (Waters), operating in positive ESI ion mode (m/z 20–500). Blanks, as well as  
185 standards of all 7 compounds obtained from Sigma-Aldrich (St. Louis, MO, USA), were run in  
186 parallel to samples. The resulting chromatograms were then used to examine the presence/absence of  
187 the target compounds in the other samples based on retention time and the mass spectra. Analyses  
188 were performed at the METABOMER platform (FR2424, Station Biologique de Roscoff).

## 189 **2.7 Statistical analyses**

190 Growth data (both algal and bacterial) were confirmed to follow a normal distribution using a  
191 Shapiro-Wilk test (Rstudio v1.0.44). Significant differences between all treatments after four weeks  
192 of co-culture (day 28) were calculated with an ANOVA and a Tukey honestly significant difference  
193 (HSD) post-hoc test with a significance level  $\alpha$  0.05 using the PAST software version 3.20 (Hammer  
194 *et al.* 2001).

## 195 **3 Results**

### 196 **3.1 Predicted metabolic interactions and selection of beneficial bacterial consortia**

197 Genome sequencing and subsequent bioinformatics analyses yielded bacterial genome assemblies  
198 with sufficient coverage and 11-72 scaffolds per genome (Table 1). Metabolic networks were then  
199 reconstructed for these ten genomes. On average, 1,714 reactions, 111 transport reactions, and 1,405  
200 metabolites (Table 2) were predicted per bacterium. These reactions belonged, again on average, to  
201 261 pathways, 137 of which were complete and 124 were incomplete (*i.e.* missing one or more  
202 reactions). Based on metabolic complementarity analysis carried out using MiSCoTo, these bacterial  
203 networks were predicted to enable the production of 160 additional compounds with the algal  
204 networks, including several polyamines (Cadaverine, Spermidine, Agmatine), amino acids (Histidine,  
205 Tyrosine, beta-alanine), vitamins B3, B9, and E, several lipids and lipid derivatives, and nucleic  
206 acids. Please refer to Supplementary Table S1 for a complete list of compounds. Many of these  
207 compounds were also previously predicted via the metabolic interaction between the same strain of  
208 *E. siliculosus* and the associated bacterium *Candidatus* Phaeomarinobacter ectocarpi (Dittami,  
209 Barbeyron, *et al.* 2014; Prigent *et al.* 2017). A total of six bacterial consortia comprising three  
210 bacterial strains each (Table 3) were predicted to be sufficient to enable the production of all of these

211 compounds. Of these six proposed consortia, two comprising one phylogenetically distinct bacterium  
212 each (i.e. the *Bacterioidetes Imperialibacter* vs the *Gammaproteobacterium Marinobacter*) were  
213 chosen for *in vivo* testing using algal-bacterial co-cultures.

### 214 **3.2 Growth rates in co-culture experiments**

215 The inoculation with one or several bacterial strains significantly enhanced algal growth by a factor  
216 of 2 compared to controls (Figure 1A). This positive effect was observed both for the predicted  
217 bacterial consortia and for all the individual strains tested. At the same time, the abundance of  
218 bacteria on algal filaments after four weeks of cultivation was significantly lower in cultures initially  
219 inoculated with bacteria compared to both controls with and without initial antibiotic treatment  
220 (Figure 1B), although bacterial cell counts in the medium were similar between co-culture  
221 experiments and the non-inoculated control after 28 days (Supplementary Figure S1).

### 222 **3.3 Bacterial impact on morphology**

223 Compared to the negative control, which exhibited a ball-like morphology typical for “axenic”  
224 cultures (Tapia *et al.* 2016), all bacterial inocula tested resulted in filamentous thalli with clear  
225 branching patterns (Figure 2). We furthermore observed differences in the branching patterns  
226 depending on the bacterial inocula. For example, *Sphingomonas*-inoculated cultures produced  
227 relatively long filaments with few branching sites (Figure 2H), whereas *Hoeflea*-inoculated cultures  
228 produced filaments with frequent branching (Figure 2E). *Imperialibacter* induced aggregation of  
229 individual filaments (Figure 2F), while in all other co-cultures, filaments remained more or less  
230 separated. These differences were, however, difficult to quantify given complexity of their  
231 morphology.

### 232 **3.4 (Algal) metabolome in co-culture conditions**

233 Seven putatively key metabolites (l-histidine, putrescine, beta-alanine, nicotinic acid, folic acid,  
234 auxin, and spermidine) predicted to be non-producible by the alga alone but producible via exchanges  
235 with some bacterial consortia, were quantified in algal tissues by UPC<sup>2</sup>-MS after four weeks of co-  
236 culture. The presence/absence of these metabolites is shown in Figure 3, comparing both the  
237 predicted producibility by metabolic network analysis and the experimental UPC<sup>2</sup>-MS results. In the  
238 negative control, i.e. antibiotic-treated algae that were not inoculated with bacteria, none of the  
239 compounds could be identified by UPC<sup>2</sup>-MS confirming the computational predictions. In contrast,  
240 in all co-cultures, at least one target compound was experimentally detected. Furthermore, each  
241 compound became producible in at least one of the co-cultures. Overall, across the 56 predictions  
242 made based on the metabolic networks (7 metabolites x 8 consortia including the individual bacteria  
243 and the negative control) *in silico* and *in vivo* data agreed in 28 cases (Figure 3). Only in four cases  
244 did we observe the presence of a metabolite although it was not predicted by the networks. Finally, in  
245 24 cases we did not detect the presence of a metabolite predicted to be producible in the co-cultures.

### 246 **3.5 Bacterial community composition after co-culture experiments**

247 The bacterial community composition of each sample was analyzed by 16S rDNA metabarcoding at  
248 the end of the co-culture experiments. This was done to verify if the bacteria inoculated had grown in  
249 the co-cultures and to determine to what extent other bacteria were present and affected by the  
250 inoculations. The results (Table 4) show that, except for *Imperialibacter*, all of the bacterial strains  
251 inoculated were detected in the corresponding co-cultures 28 days after inoculation. However, except  
252 for *Marinobacter* and *Hoeflea*, read abundances of these strains were low compared to the total

253 number of reads. In parallel, several other OTUs that had not been inoculated were detected in our  
254 co-culture experiments, suggesting that these bacteria were at least partially resistant to or protected  
255 from (*e.g.* within the cell wall) the antibiotic treatments applied, and were able to recover under the  
256 experimental conditions: in total 30 additional OTUs with a minimal abundance of 1% of total reads  
257 were detected in our samples, accounting for 63 to 82% of the total reads. Furthermore, *Hoeflea* reads  
258 were dominant in all samples including the non *Hoeflea*-inoculated cultures (14-30% of total reads).

## 259 **4 Discussion**

### 260 **Metabolic complementarity, a powerful metric despite limitations**

261 Metabolic complementarity intuitively seems like an excellent marker for beneficial metabolic  
262 interactions. The more organisms are complementary at the metabolic and by extension the gene  
263 level, the more they can potentially benefit from each other (Levy *et al.* 2015); the more they overlap  
264 in terms of metabolic pathways, the more likely they are to compete for the same resources (Kreimer  
265 *et al.* 2012). There are, however, two important restrictions that limit the applicability of this simple  
266 idea. First, the possibility of a beneficial exchange does not necessarily mean that it will occur,  
267 because this may require the presence and activation of excretion/uptake mechanisms in both  
268 partners, *e.g.* via chemical or environmental cues. Secondly, the genome-scale metabolic models used  
269 to predict metabolic complementarities may be partially erroneous and incomplete. For instance,  
270 metabolic networks frequently do not comprise interactions of chemical signals with receptor  
271 molecules, which may be key to regulate interactions (Zhou *et al.* 2016; Wang *et al.* 2018).  
272 Furthermore, in many cases, they are based on automatic predictions and annotations of protein  
273 sequences, which may, in some cases, miss genes or introduce overpredictions of functions (Schnoes  
274 *et al.* 2009). In this paper, we provide first *in vivo* tests of host-microbe interactions inferred from  
275 genome-based predictions of metabolic complementarity. Despite the aforementioned restrictions and  
276 simplifications, our results discussed below provide a strong indication that, genome-based  
277 predictions of metabolic complementarity is a powerful tool to handle the complexity of host microbe  
278 systems and to generate hypotheses on their interactions.

### 279 **Similar complementarities found across studies and *Ectocarpus* symbionts.**

280 Compared to a previous analysis of metabolic complementarity between *Ectocarpus* and another  
281 associated bacterium, *Candidatus Phaeomarinobacter ectocarpus*, (Dittami, Barbeyron, *et al.* 2014;  
282 Prigent *et al.* 2017), newly producible compounds predicted in this study were largely similar,  
283 notably regarding polyamines, histidine, beta-alanine, and auxin. This similarity persists even though  
284 metabolic complementarity analyses were performed using MiSCoTo, which incorporates the notion  
285 of different compartments minimizing the number metabolite exchanges (Frioux *et al.* 2018) and  
286 despite the fact that different bacteria were examined. The main difference compared to the previous  
287 study is that numerous additional compounds were predicted to be exchanged, which can be  
288 explained by the fact that ten rather than one bacterial network were available to complete the algal  
289 network.

### 290 **Inoculation with metabolically complementary bacteria enhances growth rate and impacts** 291 **morphology and metabolism**

292 As described above, both the bacterial consortia tested, as well as all of the bacteria inoculated  
293 individually had clear positive effects on algal growth and impacted algal morphology and metabolite  
294 profiles, even though, by the time the co-cultures were harvested, some of the inoculated bacteria  
295 were present only in very low abundance or even below the detection limit. These positive effects

296 could be due either to interactions early in the co-culture experiments followed by a decline in  
297 bacterial abundance, or due to the capacity of bacteria to impact and interact with their algal hosts  
298 even at very low cell concentrations. The latter would support the hypothesis that part of the  
299 observed effects may not be due to the exchanges of (abundant) primary metabolites, such as the  
300 predicted histidine/histidinol, but due to lowly concentrated signaling molecules or growth hormones.  
301 One such compound could be the examined auxin, which was detected in 5 of the 7 tested co-  
302 cultures, and which has previously been shown to modify the developmental patterns and  
303 morphology of *Ectocarpus* cultures (Le Bail *et al.* 2010) in a similar way as bacterial inoculations.  
304 Another observation was that the abundance of bacteria on algal filaments but not in the medium was  
305 significantly lower in co-culture conditions compared to the controls. This suggests that the  
306 inoculated bacteria, either directly, or indirectly, by stimulating algal growth or defense, can also  
307 regulate biofilm formation (see Goecke *et al.* 2010 for a review).

308 Interestingly, although differences in the effects of individual bacteria and bacterial consortia were  
309 observed on metabolite profiles and morphology, all consortia had similar effects on algal growth.  
310 Indeed, all of the tested bacteria, including *Sphingomonas*, which was not part of the minimal  
311 solutions proposed by MiSCoTo, were to a great extent complementary to the alga, already covering  
312 a large part of the metabolic gaps. In future studies, it may be particularly useful to incorporate a  
313 larger range of bacteria, possibly from other sources so that they are not expected to have evolved  
314 mutualistic interactions with brown algae. These negative controls could then be used to correlate  
315 growth rates with the presence or absence of specific metabolic capacities in the network. Once the  
316 list of candidate metabolite exchanges has been narrowed down by such comparisons, supplying  
317 these metabolites from artificial sources but also testing for their excretion into the medium by  
318 bacteria can be used to corroborate their role.

### 319 **Predicted metabolic exchanges likely to occur in part**

320 With respect to the predictions of target metabolites, we observed that for a large number of cases,  
321 predictions from the metabolic networks corresponded to the observations made by experimental  
322 metabolic profiling: none of the target metabolites were detected in the negative control, and only in  
323 four cases (Figure 3), did we detect compounds in co-cultures that were not predicted to be there.  
324 This could either be attributed to undetected metabolic pathways in the examined/added bacteria (*e.g.*  
325 due to missing annotations) or, more likely, to the activity of other bacteria present in our co-culture  
326 experiments (see below). Furthermore, there were several cases in which a potentially co-producible  
327 metabolite was not detected in our co-cultures. Here two explanations appear particularly likely: first,  
328 the metabolites in question may be produced but quickly metabolized in certain consortia, so that  
329 they do not accumulate sufficiently to be detectable in our cultures; secondly, it is possible that the  
330 corresponding biosynthetic pathway of the metabolite was not active or that the necessary exchange  
331 of metabolites was not taking place. To resolve this point in future experiments, the addition of gene  
332 expression data may help to establish whether or not biosynthetic or degradation pathways are active.  
333 From a global perspective, however, the fact that none of the compounds in question were detected in  
334 negative controls, but all of them in at least one co-culture condition, constitutes a highly promising  
335 result.

### 336 **Outlook**

337 In our opinion, the main challenge for future *in vivo* studies of metabolic complementarity will be to  
338 better control the *Ectocarpus*-associated microbiome in co-culture experiments, and thus to avoid any  
339 impact of non-inoculated microbes. The currently applied antibiotic treatments are successful in



340 removing bacteria from the algal surface to a level where they are no longer detectable by  
341 microscopy and spreading on culture medium, but once the treatment is stopped and algae are left to  
342 recover, so do parts of the microbiome, possibly from spores that were inactive or embedded in the  
343 algal cell wall and thus less susceptible to our treatments (Tetz and Tetz 2017). In the light of these  
344 results, we strongly recommend routine metabarcoding analysis for any type of coculture experiment,  
345 also in other model systems. One possibility in the future would be to use axenization protocols  
346 based on the movement of gametes, as has been done for *Ulva mutabilis* (Spoerner *et al.* 2012); at  
347 least some strains of *Ectocarpus* have previously been shown to produce phototactic gametes (Kawai  
348 *et al.* 1990). A second alternative is the continuous use of antibiotics throughout the experiment, and  
349 working with antibiotic-resistant bacterial strains. In this context a better understanding of the  
350 metabolic requirements of the algae will help to durably maintain axenic cultures.

351 Despite these challenges, the present study constitutes an important proof of concept for the use of  
352 metabolic complementarity to study simplified system of mutualistic host-symbiont interactions. We  
353 anticipate that, in the long run, this concept can be applied not only to controlled co-culture  
354 experiments, but that it will also prove useful for the interpretation of more complex datasets such as  
355 metatranscriptomic or metagenomic data.

## 356 **5 Conflict of Interest**

357 The authors declare that the research was conducted in the absence of any commercial or financial  
358 relationships that could be construed as a potential conflict of interest.

## 359 **6 Author Contributions**

360 Conceived the experiments: BB, HK, SD; Conceived in silico analyses: CF, AS. Performed  
361 experiments: BB, HK; Performed analyses: BB, ALS, EF, CF, MW, SD, EC, CL; Wrote the  
362 manuscript: SD, HK, BB. Corrected and approved of the final manuscript: all authors.

## 363 **7 Funding**

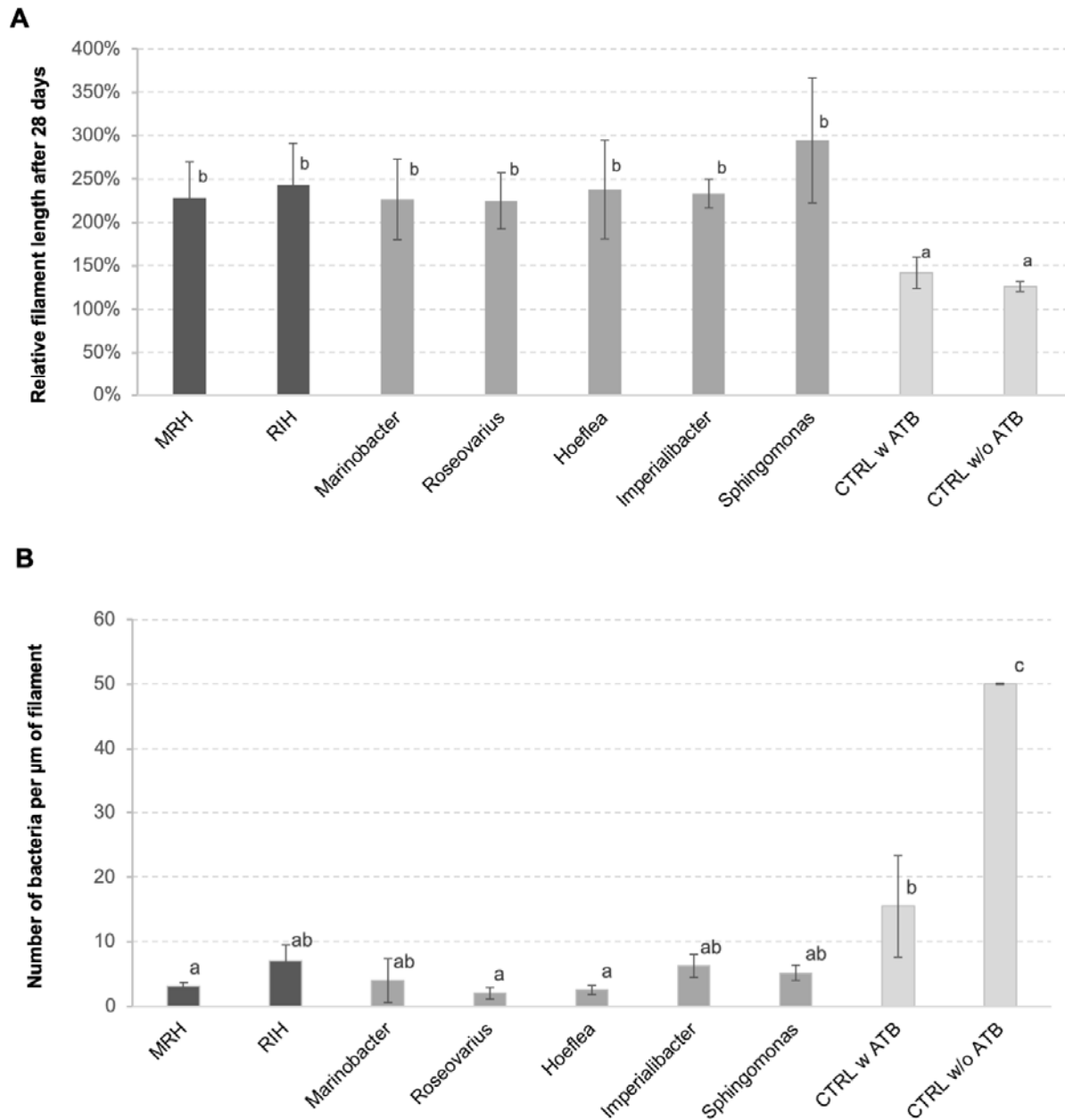
364 This work was funded partially by the CNRS Momentum call, the ANR project IDEALG (ANR-10-  
365 BTBR-04) “Investissements d’Avenir, Biotechnologies-Bioressources”, the European Union’s  
366 Horizon 2020 research and innovation Programme under the Marie Skłodowska-Curie grant  
367 agreement number 624575 (ALFF), and joint PhD scholarship from the Brittany region (Project  
368 HOSALA) and the Sorbonne University (ED227).

## 369 **8 Acknowledgments**

370 We thank Laurence Dartevelle for advice on algal culturing; Sylvie Rousvoal for extractions of  
371 bacterial DNA; Gwenn Tanguy and Erwan Legeay from the GENOMER platform (FR2424, Station  
372 Biologique de Roscoff) for access to the sequencing platform and support during library preparation;  
373 and François Thomas, Angélique Gobet, Maeva Brunet for helpful discussions and for sharing their  
374 mock community; Dominique Marie and Christian Jeanthon for granting us access to their flow  
375 cytometer; and the ABIMS platform and the GenOuest bioinformatics core facility  
376 (<https://www.genouest.org>) for providing the computing infrastructure for amplicon analyses and  
377 community predictions. The LABGeM (CEA/Genoscope & CNRS UMR8030), the France  
378 Génomique and French Bioinformatics Institute national infrastructures (funded as part of  
379 Investissement d’Avenir program managed by Agence Nationale pour la Recherche, contracts ANR-

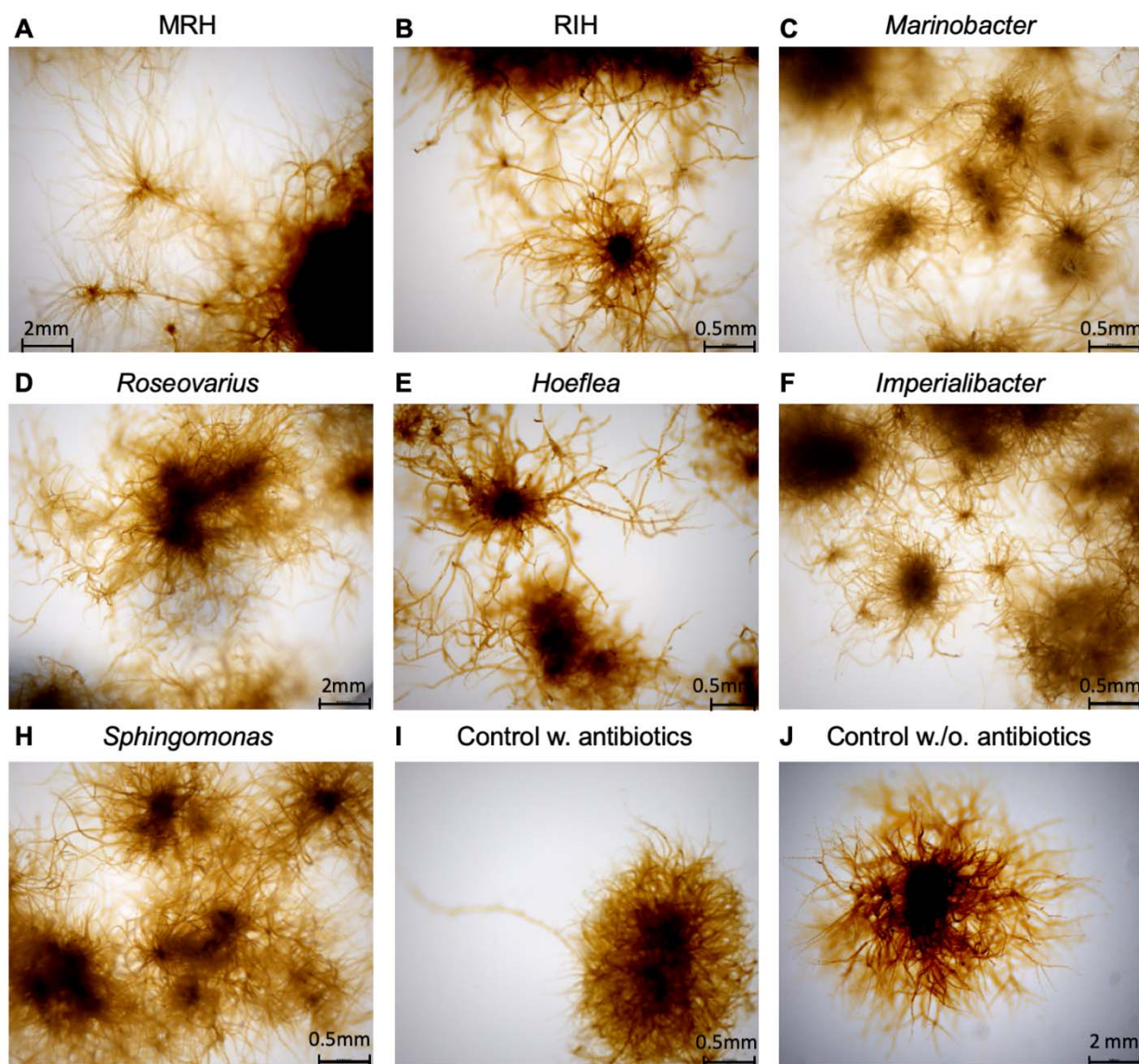
380 10-INBS-09 and ANR-11-INBS-0013) are acknowledged for support within the MicroScope  
 381 annotation platform.

382 **9 Figures**



383

384 **Figure 1:** A) Relative length of *E. siliculosus* filaments after 28 days of (co-)culture compared to the  
 385 starting point. B) Number of bacteria detected on algal filaments after 28 days of co-culture. Both  
 386 panels A and B show means of 3 replicate co-cultures  $\pm$  SD and differences are statistically  
 387 significant (one-way ANOVA  $p < 0.01$ ). The letters above the columns indicate the results of a  
 388 TUKEY HSD pairwise comparisons ( $p < 0.05$ ). CTRL = control, ATB = antibiotic treatment, MRH =  
 389 *Marinobacter-Roseovarius-Hoeflea*; RIH = *Roseovarius-Imperialibacter-Hoeflea*.



390

391 **Figure 2:** Morphological effect co-cultures with bacteria on *E. siliculosus* after 4 weeks of co-  
392 culturing. MRH = *Marinobacter-Roseovarius-Hoeflea*, RIH = *Roseovarius-Imperialibacter-Hoeflea*.

393

Target	Exchange	MRH	RIH	Marinobacter	Roseovarius	Hoeflea	Imperialibacter	Sphingomonas	CTRL w ATB
Spermidine	Dehydrosperridine	+/-	+/-	+/-	+/+	+/-	+/-	+/-	-/-
Putrescine	Agmatine	+/-	+/+	+/+	+/+	+/-	+/-	+/-	-/-
Nicotinic acid	Nicotinic acid	+/-	+/+	+/-	+/-	+/-	-/+	+/-	-/-
Folic acid	dihydrofolate	+/-	+/-	-/-	-/-	-/-	-/-	-/+	-/-
Auxine	Indole-3-acetaldehyde	+/+	+/+	-/-	-/-	-/+	+/+	-/+	-/-
L-histidine	Histidinol	+/-	+/-	+/-	+/-	+/+	+/+	+/+	-/-
Beta-Alanine	3-ureidopropanoate	+/-	+/+	+/+	+/-	+/+	+/-	-/-	-/-

394

395 **Figure 3:** Comparison of predicted production of target metabolites in co-cultures based on  
 396 metabolic networks (symbol before the slash) and results from targeted UPC<sup>2</sup>-MS analyses of algal  
 397 filaments after 28 days (symbol after the slash). The column “Exchange” indicates one possible  
 398 compound provided by the microbiome leading to the production of the compound in the column  
 399 “Target” in the algal metabolome; it was these target metabolites that were tested for using UPC<sup>2</sup>-  
 400 MS. All experiments were carried out in triplicate, each replicate of the same condition yielding  
 401 identical results. (-): a target metabolite was not predicted/detected (+): a metabolite was  
 402 predicted/detected. Green highlights conditions where predictions correspond to the in vivo  
 403 observations, red highlights compounds that were detected although no pathway was predicted.  
 404 Yellow indicates compounds potentially producible via bacterial exchanges that were not detected.  
 405 MRH: *Marinobacter-Roseovarius-Hoeflea*; RIH: *Roseovarius-Imperialibacter-Hoeflea*; CTRL =  
 406 control; ATB = antibiotic treatment.

407

## 408 10 Tables

409 **Table 1:** Overview of bacterial genomes used in this study and corresponding assembly statistics.

	raw reads	# scaffolds	genome size (mbp)	N50 (mbp)	Coverage	mapped reads
<i>Bosea</i> sp. 5A	1 863 417	26	6.34	0.98	133 X	99.91%
<i>Erythrobacter</i> sp. 430	1 065 278	11	3.14	0.44	157 X	99.93%
<i>Hoeflea</i> sp. 425	3 734 649	41	5.22	1.26	326 X	99.94%
<i>Imperialibacter</i> sp. R6	1 553 981	65	6.8	0.21	111 X	99.94%
<i>Marinobacter</i> sp. HK15	1 587 675	14	4.39	1.11	172 X	99.93%
<i>Rhizobium</i> sp. 404	1 332 560	27	4.2	0.45	148 X	99.93%
<i>Roseovarius</i> sp. 134	987 463	73	4.68	0.18	150 X	99.92%
<i>Roseovarius</i> sp. 420	803 175	85	4.68	0.12	79 X	99.89%
<i>Sphingomonas</i> sp. 631	1 111 277	25	3.28	0.29	150 X	99.87%
<i>Sphingomonas</i> sp. 391	1 150 343	74	4.6	0.16	113 X	99.91%

410

411

412

413 **Table 2:** Predicted metabolic pathways (complete pathways in parentheses), reactions and  
 414 metabolites in bacterial metabolic networks.

	number of pathways	number of reactions	transport reactions	number of metabolites
<i>Bosea</i> sp. 5A	298 (187)	1892	153	1557
<i>Erythrobacter</i> sp. 430	218 (91)	1532	63	1247
<i>Hoeflea</i> sp. 425	315 (170)	1920	129	1558
<i>Imperialibacter</i> sp. R6	239 (131)	1711	100	1425
<i>Marinobacter</i> sp. HK15	249 (128)	1679	128	1364
<i>Rhizobium</i> sp. 404	289 (142)	1814	125	1462
<i>Roseovarius</i> sp. 134	263 (146)	1703	125	1418
<i>Roseovarius</i> sp. 420	263 (143)	1701	125	1418
<i>Sphingomonas</i> sp. 361	224 (108)	1519	69	1239
<i>Sphingomonas</i> sp. 391	254 (126)	1671	92	1358

415

416 **Table 3:** Minimal bacterial consortia predicted by MiSCoTo that enabled the production of 160 algal  
 417 compounds. See Supporting table S1 for a detailed list of compounds.

Solution proposed by MiSCoTo	In vivo testing?
<i>Marinobacter</i> sp. HK15, <i>Roseovarius</i> sp. 420, <i>Hoeflea</i> sp. 425	Yes
<i>Roseovarius</i> sp. 420, <i>Imperialibacter</i> sp. R6, <i>Hoeflea</i> sp. 425	Yes
<i>Marinobacter</i> sp. HK15, <i>Bosea</i> sp. 5a, <i>Roseovarius</i> sp. 420	No
<i>Marinobacter</i> HK15, <i>Hoeflea</i> sp. 425, <i>Roseovarius</i> sp. 134	No
<i>Imperialibacter</i> sp. R6, <i>Hoeflea</i> sp. 425, <i>Roseovarius</i> sp.134	No
<i>Marinobacter</i> sp. HK15, <i>Bosea</i> sp. 5a, <i>Roseovarius</i> sp. 134	No

418

419

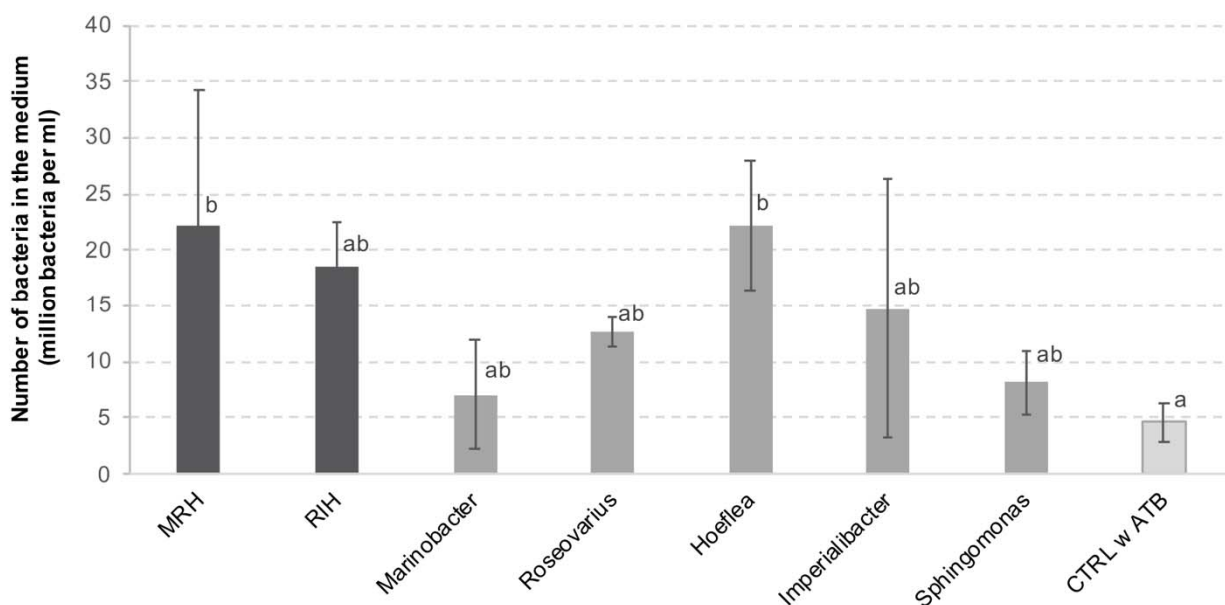
420 **Table 4:** Observed abundance of target OTUs after four weeks of co-culture. The table shows  
 421 number of reads obtained corresponding to each OTU (mean three replicates  $\pm$  SD). Bold numbers on  
 422 grey background indicate OTUs expected to be present based on the inoculations.

	MRH	RIH	<i>Marino- bacter</i>	<i>Roseo- varius</i>	<i>Hoef- lea</i>	<i>Im- periali- bacter</i>	<i>Sphing- omonas</i>	CTRL w. ATB	CTRL w./o. ATB
<i>Marinobct.O</i> TU00030	<b>82 <math>\pm</math> 48</b>	0 $\pm$ 0	<b>1103 <math>\pm</math> 1068</b>	0 $\pm$ 0	0 $\pm$ 0	0 $\pm$ 0	38 $\pm$ 38	0 $\pm$ 0	1 $\pm$ 1
<i>Roseovarius</i> OTU00055	<b>8 <math>\pm</math> 7</b>	<b>11 <math>\pm</math> 3</b>	1 $\pm$ 1	<b>41 <math>\pm</math> 10</b>	1 $\pm$ 1	0 $\pm$ 0	0 $\pm$ 0	0 $\pm$ 0	0 $\pm$ 0
<i>Hoeflea</i> OTU00001	<b>10265 <math>\pm</math> 1586</b>	<b>7644 <math>\pm</math> 889</b>	4483 $\pm$ 2777	15635 $\pm$ 1349	<b>15321 <math>\pm</math> 3515</b>	13426 $\pm$ 5338	10216 $\pm$ 4345	8899 $\pm$ 2811	3618 $\pm$ 1055
<i>Imperialib.</i> OTU00044	0 $\pm$ 0	<b>0 <math>\pm</math> 0</b>	0 $\pm$ 0	0 $\pm$ 0	0 $\pm$ 0	<b>0 <math>\pm</math> 0</b>	0 $\pm$ 0	0 $\pm$ 0	0 $\pm$ 0
<i>Sphingomn.</i> OTU00097	0 $\pm$ 0	0 $\pm$ 0	0 $\pm$ 0	0 $\pm$ 0	0 $\pm$ 0	1 $\pm$ 1	<b>4 <math>\pm</math> 4</b>	0 $\pm$ 0	0 $\pm$ 0
Other OTUs*	39403 $\pm$ 2138	23458 $\pm$ 1828	26223 $\pm$ 3187	36374 $\pm$ 7810	34190 $\pm$ 5508	38076 $\pm$ 4292	29066 $\pm$ 3302	42323 $\pm$ 9670	28009 $\pm$ 5897

423 \* see Supplementary Figure S2 for details

## 424 11 Supplementary Material

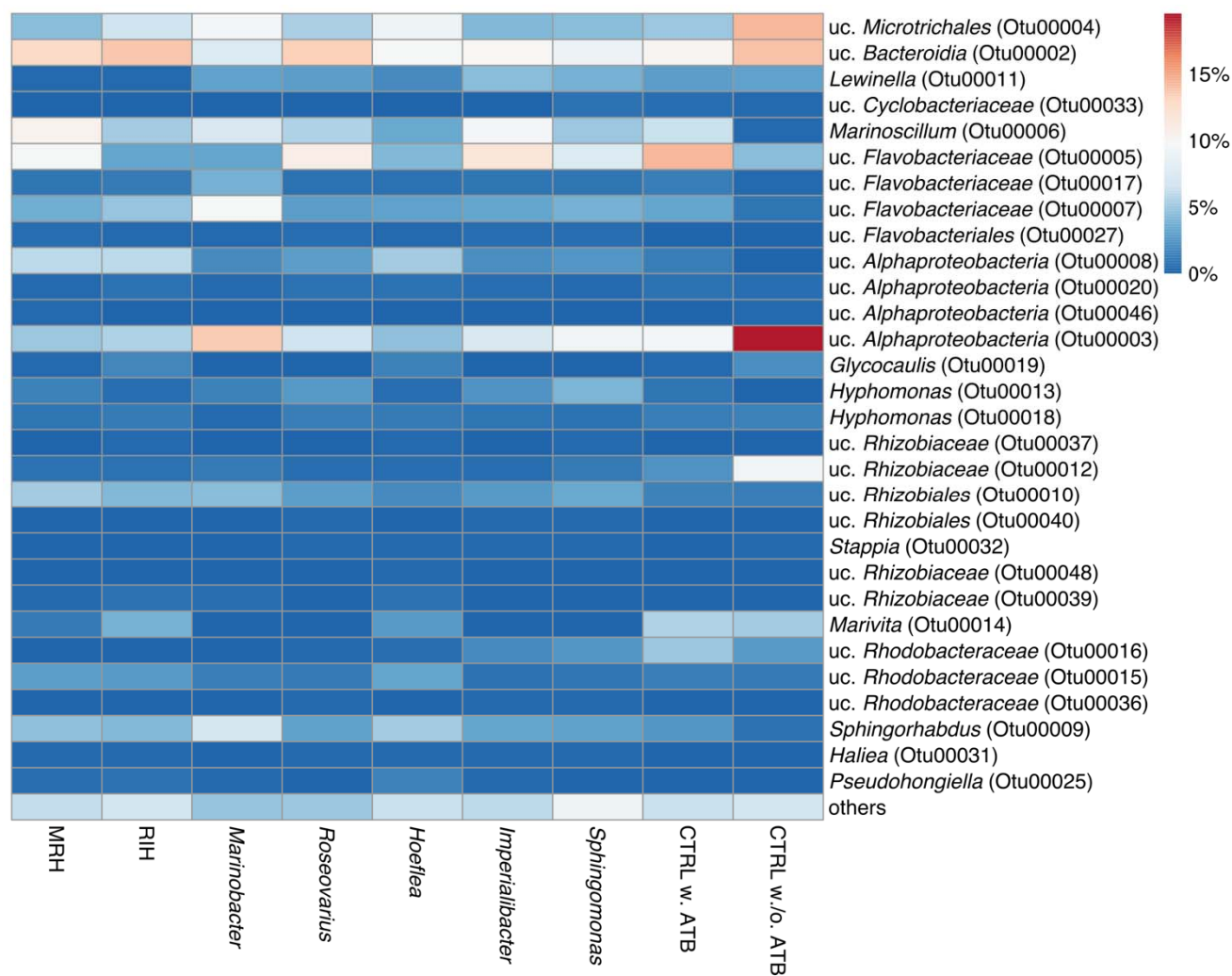
425 **Supplementary Table S1:** Metabolites predicted to become producible by the alga as a result of  
 426 metabolite exchanges between the alga and bacteria. (uploaded separately)



427

428 **Supplementary Figure S1:** Number of bacteria detected in the algal culture medium after 28 days of  
 429 co-culture. The graph shows means of 3 replicates  $\pm$  SD and differences are statistically significant  
 430 (one-way ANOVA  $p < 0.01$ ). The letters above the columns indicate the results of a TUKEY HSD  
 431 pairwise comparisons ( $p < 0.05$ ). CTRL = control, ATB = antibiotic treatment.

## Brown algal-bacterial metabolic interactions



432

433 **Supplementary Figure S2:** Heatmap of relative OTU abundance for all 30 OTUs that made up over  
 434 1% of the total number of reads and that were not inoculated (See Table 4 for the latter). This  
 435 heatmap as generated using the ClustVis service (Metsalu and Vilo 2015) using “correlation” as a  
 436 distance measure and “average linkage” as clustering method. The color code corresponds to the  
 437 mean sequence abundance for each OTU in the three replicates a percentage of total reads; uc. =  
 438 unclassified

439

440

## 441 **12 Data Availability Statement**

442 The metabarcoding data generated for this study has been deposited at the European Nucleotide  
443 Archive (ENA) under project accession number PRJEB34356. The bacterial genomes have been  
444 deposited at the ENA under the sample accessions ERZ1079053-ERZ1079062.

## 445 **13 References**

- 446 **Aite M, Chevallier M, Frioux C, et al. 2018.** Traceability, reproducibility and wiki-exploration for  
447 “à-la-carte” reconstructions of genome-scale metabolic models. *PLOS Computational Biology* **14**:  
448 e1006146.
- 449 **Amin SA, Hmelo LR, van Tol HM, et al. 2015.** Interaction and signalling between a cosmopolitan  
450 phytoplankton and associated bacteria. *Nature* **522**: 98–101.
- 451 **Aziz RK, Bartels D, Best AA, et al. 2008.** The RAST Server: rapid annotations using subsystems  
452 technology. *BMC Genomics* **9**: 75.
- 453 **Le Bail A, Billoud B, Kowalczyk N, et al. 2010.** Auxin metabolism and function in the multicellular  
454 brown alga *Ectocarpus siliculosus*. *Plant Physiology* **153**: 128–44.
- 455 **Bankevich A, Nurk S, Antipov D, et al. 2012.** SPAdes: a new genome assembly algorithm and its  
456 applications to single-cell sequencing. *Journal of Computational Biology* **19**: 455–77.
- 457 **Bligh EG, Dyer WJ. 1959.** A rapid method of total lipid extraction and purification. *Canadian*  
458 *Journal of Biochemistry and Physiology* **37**: 911–917.
- 459 **Bolger AM, Lohse M, Usadel B. 2014.** Trimmomatic: a flexible trimmer for Illumina sequence data.  
460 *Bioinformatics* **30**: 2114–20.
- 461 **Dittami SM, Barbeyron T, Boyen C, et al. 2014.** Genome and metabolic network of “Candidatus  
462 Phaeomarinobacter ectocarpi” Ec32, a new candidate genus of *Alphaproteobacteria* frequently  
463 associated with brown algae. *Frontiers in Genetics* **5**: 241.
- 464 **Dittami SM, Eveillard D, Tonon T. 2014.** A metabolic approach to study algal-bacterial  
465 interactions in changing environments. *Molecular ecology* **23**: 1656–60.
- 466 **Frioux C, Fremy E, Trottier C, Siegel A. 2018.** Scalable and exhaustive screening of metabolic  
467 functions carried out by microbial consortia. *Bioinformatics* **34**: i934–i943.
- 468 **Goecke F, Labes A, Wiese J, Imhoff J. 2010.** Chemical interactions between marine macroalgae  
469 and bacteria. *Marine Ecology Progress Series* **409**: 267–299.
- 470 **Hammer Ø, Harper D, Ryan P. 2001.** PAST: Paleontological statistics software package for  
471 education and data analysis. *Palaeontologia Electronica* **4**.
- 472 **Illumina. 2017.** *16S Metagenomic Sequencing Library Preparation*.  
473 [https://support.illumina.com/documents/documentation/chemistry\\_documentation/16s/16s-](https://support.illumina.com/documents/documentation/chemistry_documentation/16s/16s-metagenomic-library-prep-guide-15044223-b.pdf)  
474 [metagenomic-library-prep-guide-15044223-b.pdf](https://support.illumina.com/documents/documentation/chemistry_documentation/16s/16s-metagenomic-library-prep-guide-15044223-b.pdf).



- 475 **Karp PD, Latendresse M, Paley SM, et al. 2016.** Pathway Tools version 19.0 update: software for  
476 pathway/genome informatics and systems biology. *Briefings in Bioinformatics* **17**: 877–890.
- 477 **Kawai H, Müller DG, Fölster E, Häder D-P. 1990.** Phototactic responses in the gametes of the  
478 brown alga, *Ectocarpus siliculosus*. *Planta* **182**: 292–7.
- 479 **KleinJan H, Jeanthon C, Boyen C, Dittami SM. 2017.** Exploring the cultivable *Ectocarpus*  
480 microbiome. *Frontiers in Microbiology* **8**: 2456.
- 481 **Kozich JJ, Westcott SL, Baxter NT, Highlander SK, Schloss PD. 2013.** Development of a dual-  
482 index sequencing strategy and curation pipeline for analyzing amplicon sequence data on the miseq  
483 illumina sequencing platform. *Appl. Environ. Microbiol.* **79**: 5112–5120.
- 484 **Kreimer A, Doron-Faigenboim A, Borenstein E, Freilich S. 2012.** NetCmpt: a network-based tool  
485 for calculating the metabolic competition between bacterial species. *Bioinformatics* **28**: 2195–2197.
- 486 **Levy R, Carr R, Kreimer A, Freilich S, Borenstein E. 2015.** NetCooperate: a network-based tool  
487 for inferring host-microbe and microbe-microbe cooperation. *BMC Bioinformatics* **16**: 164.
- 488 **Lindemann SR, Bernstein HC, Song H-S, et al. 2016.** Engineering microbial consortia for  
489 controllable outputs. *The ISME journal* **10**: 2077–84.
- 490 **Masella AP, Bartram AK, Truszkowski JM, Brown DG, Neufeld JD. 2012.** PANDAseq: paired-  
491 end assembler for illumina sequences. *BMC bioinformatics* **13**: 31.
- 492 **Metsalu T, Vilo J. 2015.** ClustVis: a web tool for visualizing clustering of multivariate data using  
493 Principal Component Analysis and heatmap. *Nucleic Acids Research* **43**: W566–W570.
- 494 **Prigent S, Collet G, Dittami SM, et al. 2014.** The genome-scale metabolic network of *Ectocarpus*  
495 *siliculosus* (EctoGEM): a resource to study brown algal physiology and beyond. *Plant Journal* **80**:  
496 367–381.
- 497 **Prigent S, Frioux C, Dittami SM, et al. 2017.** Meneco, a Topology-Based Gap-Filling Tool  
498 Applicable to Degraded Genome-Wide Metabolic Networks. *PLOS Computational Biology* **13**:  
499 e1005276.
- 500 **Rohwer F, Seguritan V, Azam F, Knowlton N. 2002.** Diversity and distribution of coral-associated  
501 bacteria. *Marine Ecology Progress Series* **243**: 1–10.
- 502 **Schnoes AM, Brown SD, Dodevski I, Babbitt PC. 2009.** Annotation error in public databases:  
503 misannotation of molecular dunction in enzyme superfamilies. *PLoS Computational Biology* **5**:  
504 e1000605.
- 505 **Spoerner M, Wichard T, Bachhuber T, Stratmann J, Oertel W. 2012.** Growth and thallus  
506 morphogenesis of *Ulva mutabilis* (Chlorophyta) depends on a combination of two bacterial species  
507 excreting regulatory factors. *Journal of Phycology* **48**: 1433–1447.
- 508 **Tapia JE, González B, Goulitquer S, Potin P, Correa JA. 2016.** Microbiota Influences  
509 Morphology and Reproduction of the Brown Alga *Ectocarpus* sp. *Frontiers in Microbiology* **7**: 197.
- 510 **Tetz G, Tetz V. 2017.** Introducing the sporobiota and sporobiome. *Gut pathogens* **9**: 38.

- 511 **Thomas F, Dittami SM, Brunet M, et al.** Evaluation of a new primer combination to minimize  
512 plastid contamination in 16S rDNA metabarcoding analyses of alga-associated bacterial  
513 communities. *Environmental Microbiology Reports* **in prep**.
- 514 **Vallenet D, Labarre L, Rouy Z, et al. 2006.** MaGe: a microbial genome annotation system  
515 supported by synteny results. *Nucleic Acids Research* **34**: 53–65.
- 516 **Wahl M, Goecke F, Labes A, Dobretsov S, Weinberger F. 2012.** The second skin: ecological role  
517 of epibiotic biofilms on marine organisms. *Frontiers in Microbiology* **3**: 292.
- 518 **Wang Q, Garrity GM, Tiedje JM, Cole JR. 2007.** Naive Bayesian classifier for rapid assignment  
519 of rRNA sequences into the new bacterial taxonomy. *Applied and Environmental Microbiology* **73**:  
520 5261–7.
- 521 **Wang Q, Liu J, Zhu H. 2018.** Genetic and molecular mechanisms underlying symbiotic specificity  
522 in legume-*Rhizobium* interactions. *Frontiers in Plant Science* **9**: 313.
- 523 **Zhou J, Lyu Y, Richlen ML, Anderson DM, Cai Z. 2016.** Quorum sensing is a language of  
524 chemical signals and plays an ecological role in algal-bacterial interactions. *Critical Reviews in Plant*  
525 *Sciences* **35**: 81–105.
- 526